



D5.2 – Global BIG-MAP experimental matrix, proof-of-concept of BIG-MAP experimental workflow and definition of perspectives and future vision towards the European multi-modal platform.

VERSION

VERSION	DATE
1	31/01-2024

PROJECT INFORMATION

GRANT AGREEMENT NUMBER	957189
PROJECT FULL TITLE	Battery Interface Genome - Materials Acceleration Platform
PROJECT ACRONYM	BIG-MAP
START DATE OF THE PROJECT	1/9-2020
DURATION	3 years
CALL IDENTIFIER	H2020-LC-BAT-2020-3
PROJECT WEBSITE	big-map.eu

DELIVERABLE INFORMATION

WP NO.	5
WP LEADER	S. Lyonnard (CEA)
CONTRIBUTING PARTNERS	CEA, ESRF
NATURE	Report
AUTHORS	Q. Jacquet, S. Lyonnard, F. Cadiou, D. Blanchard
CONTRIBUTORS	E. Flores, S. Clark, C. Herrera, N. Mozhzhukhina. All partners of WP5 for constructing the global experimental matrix and participating in the workflows.
CONTRACTUAL DEADLINE	31/01-2024
DELIVERY DATE TO EC	31/01-2024
DISSEMINATION LEVEL (PU/CO)	PU

ACKNOWLEDGMENT



This project has received funding from the European Union's Horizon 2020 research and innovation programme under grant agreement No 957189. The project is part of BATTERY 2030+, the large-scale European research initiative for inventing the sustainable batteries of the future.



ABSTRACT

D5.2. entitled "Global BIG-MAP experimental matrix, proof-of-concept of BIG-MAP experimental workflow and definition of perspectives and future vision towards the European multi-modal platform" gathers three different parts (1) the experimental matrix, (2) establishment of characterisation workflows and (3) perspectives.

The global experimental matrix is reported here. It is a database of 136 techniques available in the BIG-MAP consortium, together with their 28 technical characteristics (resolution, observables, etc.) and logistical information (availability, point of contact, etc.) needed to build efficient workflows. This database should help the battery community to select the most appropriate techniques and experts for their needs. Along that line, a user-friendly graphical interface of the global experimental matrix database has been demonstrated, with help from WP7, allowing to search through the matrix using natural language-based queries.

A characterisation workflow is essentially a method to acquire correlated datasets. D5.2 describes three main workflow strategies adopted in WP5: (1) using and developing new multi-probe techniques capable of measuring several observables at the same time and on the same sample, (2) building multi-technique workflows in which a limited number of partners measure standard samples to answer a limited set of scientific questions and (3) large multi-technique workflows in which every partner measures standard samples to tackle a large set of scientific questions.

Finally, looking back on the WP5 experience, several future perspectives for the European multi-modal platform are defined:

- Using the global experimental matrix to build an automatic workflow builder app, the algorithm would be constructed based on D5.3 and D5.5.
- Extend workflows and global experimental matrix to new chemistries and cell format.
- Continue to develop new access modes for large-scale facilities to ensure that these powerful characterisation facilities can participate efficiently in workflows.
- Push correlated data analysis by designing news tools or bringing existing tools into the battery community.



TABLE OF CONTENTS

1. GENERAL INTRODUCTION	4
2. GLOBAL EXPERIMENTAL MATRIX	4
2.1 INTRODUCTION	4
2.2 CONTENT OF THE GLOBAL MATRIX	4
2.3 FORMAT OF THE MATRIX.....	6
2.4 CONCLUSIONS AND PERSPECTIVES.....	7
3. PROOF-OF-CONCEPT OF BIG-MAP EXPERIMENTAL WORKFLOW	7
3.1 INTRODUCTION	7
3.2 NEW TECHNIQUES TOWARDS CORRELATIVE CHARACTERIZATION: OPERANDO OEMS AND WAXS/SAXS MICROBEAM MAPPING	8
3.2.1 SCIENTIFIC CASE	9
3.2.2 CORRELATING LOCAL STRUCTURAL AND GAS EVOLUTION: OPERANDO OEMS AND WAXS/SAXS MAPPING.....	9
3.2.3 CONCLUSION & PERSPECTIVE	10
3.3 ATOMIC AND ELECTRONIC STRUCTURE OF LiNiO_2 PROBED BY MULTI - TECHNIQUE SPECTROSCOPIES.....	11
3.3.1 SCIENTIFIC CASE	11
3.3.2 MULTIPLE DATASETS IN INTERACTION WITH ATOMISTIC MODELLING	11
3.3.3 CONCLUSIONS & PERSPECTIVES	12
3.4 DEMONSTRATION OF THE CAPABILITY TO RUN COORDINATED MULTI-TECHNIQUES EXPERIMENTS TO ACQUIRE MULTI-SCALE DATA, AND PRACTICAL APPLICATION TO A SELECTED CHEMISTRY (D5.3).....	13
4. DEFINITION OF PERSPECTIVES AND FUTURE VISION TOWARDS THE EUROPEAN MULTI-MODAL PLATFORM.....	13
4.1 INTRODUCTION	13
4.2 TOWARDS AN AUTOMATIC WORKFLOW BUILDER.....	13
4.3 EXPENDING WORKFLOWS TOWARDS CHEMISTRY NEUTRALITY.....	14
4.4 NEW ACCESS MODE TO LARGE-SCALE FACILITIES TO FACILITATE THE INTEGRATION OF THESE TOOLS INTO EFFICIENT WORKFLOWS.....	15
4.5 STRATEGIES TO IMPROVE DATA CORRELATION	16



1. General introduction

D5.2 is the final deliverable of WP5 – a work package dedicated to characterisation - will cover two important aspects of WP5 work:

- The experimental matrix is a database of techniques available in the BIG-MAP consortium and their technical specificities.
- Demonstration of different types of workflow strategies conducted in WP5 with specific examples (sequence of characterisations with correlated datasets) in line with the key demonstrator “Multi-modal characterization demonstrator capable of running coordinated multi-technique experiments to acquire multi-scale/multi-fidelity data”.

Finally, critically looking back on WP5, perspectives will be proposed for the following challenges to the implementation of a European multi-modal experimental platform using standardized cells/protocols/metadata/data collection, treatment, and analysis.

2. Global experimental matrix

2.1 Introduction

The global experimental matrix consists of a database gathering all information needed to build characterization workflows (sequence of characterisation experiments producing correlated datasets). The matrix aims to be exhaustive in terms of techniques, including both laboratory and large-scale facilities (LSF). For each technique, technical characteristics (resolution, length and time scales, etc.) and organisational information (fidelity, planning time, contact point, etc.) are defined and reported by WP5 experts in agreement with WP7 and WP8 standards. Moreover, beyond the scope described in the project, we built, with help from WP7, the first steps towards a graphical interface to consult the global experimental matrix using a simple natural language-based questionnaire. This tool is not yet fully operational and, hence, is unavailable in its current state.

In the following, we will describe the content of the global experimental matrix along with developments regarding user-friendly ways to read the matrix. Note that parts of the matrix are shown in Figure 1, Figure 2, and Figure 3 and that the entire matrix is available online at the [BIG-MAP website](#).

2.2 Content of the global matrix

The global experimental matrix has been built on the matrix reported in D5.1 and delivered in month 6. This matrix already contained a list of available characterisation techniques in the consortium and some of their technical characteristics (observables, resolution, probed region, etc.) and contact points.

The global experimental matrix content contains two major improvements.

- The technical details and technique list have been updated, reaching 136 techniques. Note that technical characteristic entries match the BIG-MAP Notebook developed by WP8 (OLN - <http://big-map-notebook.u-picardie.fr>).



- While designing workflows, extra information regarding logistics and technique ease was added, reaching up to 28 characteristics for each technique. We have introduced the Characterisation Readiness Level (CRL) in more detail. CRL is proposed to inform on the challenge to obtain the desired observable using a selected technique successfully. CRL is based on expert appreciation (Low/Medium/High) as an indication to non-expert users. For example, determining crystallographic unit cell parameters using laboratory X-ray diffraction, synchrotron microbeam X-ray diffraction, and synchrotron X-ray nano-diffraction would have acquisition CRL of High, Medium, and Low, respectively.
- Moreover, we defined a separate CRL for data analysis. Indeed, despite the general trend that improvements in acquisition and analysis come hand in hand, there are enough examples of deviations to justify the separation of both CRLs (for example, some synchrotron experiments can be challenging to perform with relatively straightforward data analysis). Moreover, logistical information was included: degree of fidelity, maturity, resources, planning time, post-processing time, use in BIG-MAP, sample reuse, and data analysis software. Most of them are self-explanatory except perhaps for the degree of fidelity (how accurate is the obtained observable – see D11.1) and resources (Cheap/Medium/Expensive – estimated cost including consumable and manpower).

Cluster	Partner	technique	probed area	probed area resolution	penetration depth	permenetration depth resolution	detection limit	detection limit Resolutio	contrast
Diffraction	[DTU]	[X-ray diffraction, XRD]	[few mm2]	[Null]	[mm, cm]	[Null]	[crystallinity (> 5 nm cryst. size)]	[1-2 wt.%]	[atomic number contrast]
Diffraction	[ESRF]	[X-ray diffraction, XRD]	[few mm2]	[Null]	[cm]	[Null]	[crystallinity (> 5 nm cryst. size)]	[1-2 wt.%]	[atomic number contrast]
Diffraction	[CEA]	[Neutron Diffraction, ND]	[up to 3x5 cm2]	[5 mm]	[cm]	[Null]	[crystallinity (> 5 nm cryst. size)]	[1-2 wt.%]	[Neutron scattering contrast]
Diffraction	[ILL]	[Neutron Diffraction, ND]	[up to 3x5 cm2]	[1 mm]	[cm]	[Null]	[crystallinity (> 5 nm cryst. size)]	[1-2 wt.%]	[Neutron scattering contrast]
Diffraction	[TUD]	[Neutron Diffraction, ND]	[up to 3x5 cm2]	[1 mm]	[cm]	[Null]	[crystallinity (> 5 nm cryst. size)]	[1-2 wt.%]	[Neutron scattering contrast]
Diffraction	[TUD]	[Laboratory X-ray Diffraction, lab XRD]	[1 to 50 mm2]	[Null]	[101 μm with Cu (8 keV), 1 mm with Mo (17.45 keV)]	[Null]	[crystallinity (> 5 nm cryst. size)]	[1-2 wt.%]	[atomic number contrast]
Diffraction	[CEA]	[Laboratory X-ray Diffraction, lab XRD]	[1 to 50 mm2]	[cm]	[101 μm with Cu (8 keV), 1 mm with Mo (17.45 keV)]	[Null]	[crystallinity (> 5 nm cryst. size)]	[1-2 wt.%]	[atomic number contrast]
Diffraction	[DTU]	[Laboratory X-ray Diffraction, lab XRD]	[1 to 50 mm2]	[Null]	[101 μm with Cu (8 keV)]	[Null]	[crystallinity (> 5 nm cryst. size)]	[1-2 wt.%]	[atomic number contrast]

Figure 1. 1-10/28 columns (characteristics) and 1-10/136 lines (techniques) of the global experimental matrix (note that the contact column is not shown).

observables	Observables resolution	characterization mode	time scale	Sample preparation	Instrument	Beam source	Cell Availability	Degree of fidelity	Maturity
[crystal structure, phase fractions, crystallite morphology, strain]	[High/Medium/Low]	[Ex-situ/m-situ/Operando]	[ms, min]	[Cylindrical cell, Pouch cell]	[Null]	[Synchrotron]	[Yes/no]	[Low/medium/high/best]	[Commercial/Realistic/Model]
[crystal structure, phase fractions, crystallite morphology, strain]	[Null]	[Ex-situ, operando]	[ms, min]	[transmission geometry, reflection geometry, CR20XX coin cell, swagelok type cell]	[ID22, ID31]	[Synchrotron]		[Best]	[Commercial]
[crystal structure, phase fractions, crystallite morphology, strain]	[H,H,L,M]	[Ex-situ, operando]	[min]	[Model Cell, Cylindrical cell, Pouch cell]	[D20, D19]	[Neutron]	[Yes]	[High]	[Commercial]
[crystal structure, phase fractions, crystallite morphology, strain]	[High]	[Ex-situ, operando]	[ms, min]	[ILL operando cells]	[D28, D20, D19]	[Neutron]	[Yes]	[High/best]	[Commercial]
[crystal structure, phase fractions, crystallite morphology, strain]	[Null]	[Ex-situ, operando]	[ms, min]	[Null]	[PEARL]	[Neutron]		[High/best]	[Commercial]
[crystal structure, phase fractions, crystallite morphology, strain]	[Null]	[Ex-situ, operando]	[5 < Δt < 30 mins]	[Kapton-window cell, gas connections, reflection geometry]	[Null]	[Cu, Co, Mo, Ag]		[High]	[realistic]
[crystal structure, phase fractions, crystallite morphology, strain]	[M, H, L, M]	[Ex-situ, operando]	[5 < Δt < 30 mins]	[Be windows, coin cells]	[Bruker D8 Advance]	[Cu, Mo]	[Yes]	[High]	[realistic]
[crystal structure, phase fractions, crystallite morphology, strain]	[Null]	[Ex-situ, operando]	[5 < Δt < 30 mins]	[ELCELL, reflection geometry]	[Null]	[Cu]	[Yes]	[High]	[realistic]

Figure 1. 10-20/28 columns (characteristics) and 1-10/136 lines (techniques) of the global experimental matrix (note that the contact column is not shown).



Resources	Planning time	Post-processing time	CRL by observable Acquisition	CRL by observable analysis	used in BIG-map	Sample reuse	Data analysis Software
Cheap/Medium/Expensive	Hours/Days/Weeks/Months	Hours/Days/Weeks/Months	High-Medium-Low	High-Medium-Low	Yes/No	Yes/No	Inhouse/commercial/opensource/name
[Expensive]	[Months]	[Hours/Days]	[High]	[Medium]	[Yes]	[Yes]	[Commercial (Topas), free (Fullprof)]
[Expensive]	[Months]	[Hours/Days]					
[Expensive]	[Months]	[Hours/Days]	[High, High, Medium, High]	[High, High, Medium, High]	[yes]	[yes]	[FullProf]
[Expensive]	[Months]	[Hours/Days]	[High, High, Medium, High]	[High, High, Medium, High]	[Yes]	[Yes]	[FullProf]
[Expensive]	[Months]	[Hours/Days]					
[Cheap]	[Hours]	[Hours/Days]					
[Cheap]	[Hours]	[Hours/Days]	[High, High, Medium, High]	[High, High, Medium, High]	[no]	[yes]	[Fullprof]
[Cheap]	[Hours]	[Hours/Days]	[High]	[High]	[Yes]	[No]	[Commercial (Topas), free (Fullprof)]

Figure 2. 20-28/28 (characteristics) and 1-10/136 lines (techniques) of the global experimental matrix (note that the contact column is not shown).

2.3 Format of the matrix

We rapidly realized that the matrix's necessary level of detail and complexity were making it very difficult to read, especially for non-expert users. Therefore, the shape of the matrix has been revised to build a graphical interface for interrogating its content (Collab. with E. Flores and S. Clark from SINTEF – WP7). The interface has been designed to be user-friendly with one natural language entry. This is based on an underlying Large Language Model (LLM), a type of AI model similar to that powering ChatGPT, that translates this question into a computer-readable formatted query to retrieve the information from the global experimental matrix. As showcased in the example in Figure 4, it provides a simple and intuitive way to interrogate the experimental matrix. This is still a prototype and has evident drawbacks (questions with words not precisely matching the matrix entries or with too many criteria might not be correctly understood, etc.). The answers can be made more accurate by, for instance, fine-tuning the LLMs to an authoritative scientific corpus or by engineering prompts to improve the ability of the model to find the right content. In any case, we believe this is an interesting proof of concept that could help many non-expert users understand which techniques could be the most appropriate and who to contact for access or further information.

Tabular Data Question Answering

Ask your question

which techniques has the CEA partner made available in the consortium?

Neutron Diffraction and ND, Laboratory X-ray Diffraction and lab XRD, Synchrotron X-ray diffraction and synchrotron XRD

Advanced result

Examples

Table

Figure 3. Example of the graphical interface to query the experimental matrix.

2.4 Conclusions and perspectives

The global experimental matrix was successfully assembled, gathering 136 techniques available in the BIG-MAP consortium. Each technique is described according to 28 technical and logistical characteristics. In terms of perspectives, the table should be kept alive. Its content is updated with newly available techniques coming from either new instruments or new partners (opening beyond the BIG-MAP consortium to Europe, for example) and data following technical development in each technique (for example, data analysis can become more robust or faster with software development or instrument specificities can evolve).

3. Proof-of-concept of BIG-MAP experimental workflow

3.1 Introduction

The objective of WP5 was to set up and perform characterization workflows. These are sets of characterisation experiments planned and executed to correlate the acquired datasets (i.e., same samples, same conditions, same technique list with different samples, etc.). Moreover, the rest of the consortium should use the collected data and comply with standardized methodology/format/protocols defined in WP7 and WP8. Additionally, data acquisition and/or analysis can be aided by AI modules (WP10) and modelling (WP2, WP3, and WP11). Practical validation of WP5 workflows has been performed on selected chemistry using a sub-set of key techniques. The ambition of WP5 is to design workflows combining lab and large-scale facility techniques probing electrochemical, chemical, electronic, structural, and morphological properties at multiple scale levels (materials, interfaces, components, and cells). To produce and perform these workflows, three different strategies were tested, for which we selected representative examples (more examples can be found in D5.3 and D5.4):



- (1) It is building new techniques capable of combining several probes on the same instrument that directly provides correlated datasets: “Operando OEMS and WAXS/SAXS microbeam mapping to understand the effect of overcharge on spatial heterogeneities”.
- (2) Smaller workflows are limited to a few relevant and new techniques to answer a specific scientific question: “Atomic and electronic structure of LiNiO_2 probed by multiple bulk spectroscopies”.
- (3) A general workflow including a large number of partners, techniques, and spatial and temporal scales answering broader scientific questions: “What is the effect of LiTDI during the LNO/Gr full cell aging on the atomic and electronic structure, morphology, surface, gas production, and Li heterogeneities?”.

Before digging into the selected examples, we want to emphasize that WP5 has produced large datasets that cannot all be presented in this work. For example, studies on LNO include:

- Structural evolution investigation during cycling (operando) over different length scales (averaged over the entire electrode using operando lab XRD, at the electrode scale with in-depth and in-plane resolution using operando synchrotron micro X-ray diffraction, and at the single particle scale with X-ray nano diffraction).
- Bulk and surface spectroscopic investigations and gas evolution are exemplified in sections 3.2 and 3.3.
- Li dynamics were investigated during cycling at the atomic scale using operando and ex situ NMR and electrode scale using operando neutron imaging and ex situ neutron depth profiling.
- Imaging at the micro, nano, and atomic scale is performed using ex situ micro and nano X-ray tomography, scanning electron microscopy, and transmission electron microscopy.

3.2 New techniques towards correlative characterization: Operando OEMS and WAXS/SAXS microbeam mapping

The essence of WP5 workflows is to correlate characterization data. This can be done by having standard samples shipped to different partners and measured independently. Although simple, this approach has drawbacks: (1) air exposure during in-sample transfer might compromise reproducibility, (2) it can be difficult to exactly reproduce cycling conditions between multiple operando experiments due to the difference in operando cell designs and/or external parameters (temperature, time between sample fabrication and measurement, etc.), (3) spatial and temporal correlations might not be possible with two different samples. Therefore, it is advantageous to perform characterization experiments with the same instrument and hence on the same sample, at the same position in the sample, and at the same time. Towards this end, we have developed new multi-modal experiments directly combining several techniques. For example, we have performed a combined operando online electrochemical mass spectrometry (OEMS) with wide-angle X-ray scattering and small-angle X-ray scattering (WAXS/SAXS) mapping, which enabled a direct correlation between gas production and local state of charge in a single layer LiNiO_2 (BASF)/Graphite Silicon (GrSi - CIDETEC) pouch cell.



3.2.1 Scientific case

The degradation mechanisms in Li-ion batteries are very complex, characterized by numerous dynamic processes occurring over multiple length scales and involving multiple components. Hence, gathering as much information as possible simultaneously and across different scales is crucial. In the following, we focus on degradation s involving gas production and leading to heterogeneous reactions.

Some LNO and GrSi degradation mechanisms involve gas formation, especially during high voltage operation and/or overcharge (oxygen loss from LNO and constant SEI formation on Si)¹. Concerning this aspect, CEA and UCAM have conducted gas analysis using OEMS on standard BIG-MAP materials (LNO from BASF and Gr or GrSi from CIDETEC) but also on LNO-coated samples prepared in WP4 or using advanced electrolytes developed in WP6. In both cases, the coating and the advanced electrolytes resulted in a reduction of gas production correlated with better cycling performance in realistic cells.

Degradation mechanisms due to fast charging and aging induce stronger reaction heterogeneities inside commercial cells. Indeed, DTU demonstrated increased reaction heterogeneity in prismatic NMC/GrSi cells after aging.

Until now, there have been no reports interrogating the influence of overcharge on reaction heterogeneity and, hence, the possible correlation between gas production and reaction heterogeneity. Therefore, CEA designed a combined operando OEMS and WAXS/SAXS mapping experiment to probe the formation cycle and overcharge of an LNO/GrSi pouch cell.

3.2.2 Correlating local structural and gas evolution: operando OEMS and WAXS/SAXS mapping

This work reports the simultaneous measurement of gas production and mapping of active material structural evolution in a single-layer pouch cell during the formation cycle and overcharge, as shown in Figure 5. In short, an LNO/GrSi pouch cell is connected to a mass spectrometer to measure the amount and chemical nature of the gases that are produced. Simultaneously, the entire pouch is scanned with a synchrotron X-ray microbeam during cycling, and both wide and small-angle X-ray scattering signal is measured, leading to 4D datasets (2D images composed of a WAXS and SAXS pattern for each pixel). The experiment was a success, and the beam effect was measured to be negligible. Indeed, the electrochemistry, average diffraction pattern, and gas evolution were comparable to the ones obtained in the consortium (pouch and coin cell performed by CEA, operando XRD/SXRD from DTU/CEA, and OEMS from CEA/UCAM). In terms of results, first, a direct correlation was found between the structural evolution of both electrodes obtained by diffraction (WAXS) and the gas release. CO₂ and O₂ production occur at the end of the H2-H3 transition without O1 phase formation. Second, by spatially resolving the cell parameter changes in the pouch, in-plane heterogeneities in both electrodes are quantified and found to originate from three sources: (1) edge effects due to an oversized GrSi electrode, (2) position of the current collector tabs and (3) the overcharge. Indeed, the discharge after the overcharge features very local regions below 1 mm diameter, lagging behind the overall electrochemistry. Some of these positions correspond to visible fabrication defects of the pouch. We propose that gas bubbles formed during the overcharge gather at cell defects, inducing the observed heterogeneity¹³.

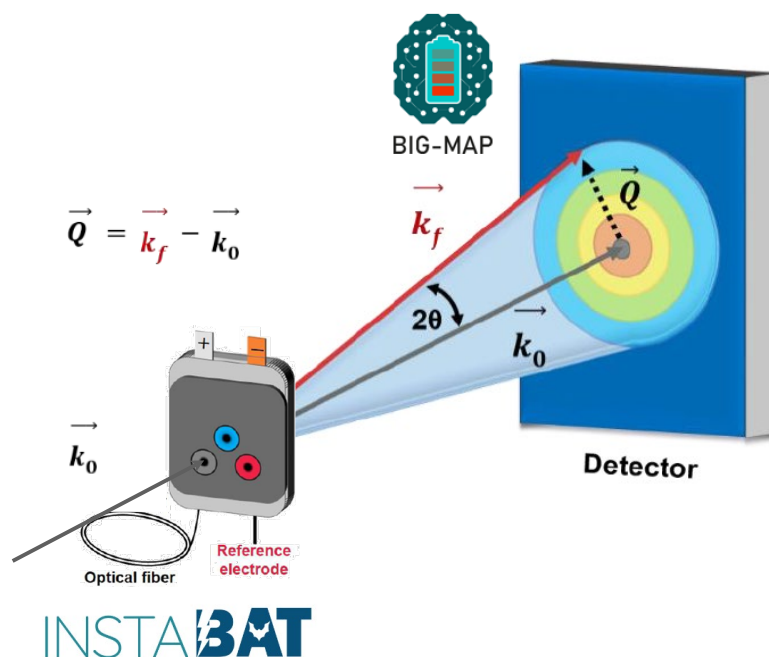


Figure 5. Schematic of a fiber-equipped prismatic cell designed in INSTABAT project measured at the synchrotron using WAXS mapping in the context of BIG-MAP.

3.3 Atomic and electronic structure of LiNiO_2 probed by multi-technique spectroscopies

Several partners and techniques were bridged to understand the intriguing atomic and electronic structure of LiNiO_2 . All partners used BIG-MAP LiNiO_2 electrodes provided by BASF, using WP8-defined standard conditions for experiments when possible.

3.3.1 Scientific case

LiNiO_2 is a promising cathode material for Li-ion batteries with a complex structure and dynamics. Local structural characterisation techniques such as X-ray absorption spectroscopy and neutron total scattering proved that there are two types of Ni-O bonds, two long and four short bonds (2.05 and 1.92 Å, respectively). However, such distortion is not observed on neutron or X-ray diffraction patterns, indicating its non-cooperative nature for which different theories have been recently proposed: (1) high entropy charge and bond disproportionation due to negative charge transfer, (2) dynamic bond disproportionation, (3) static disordered Jahn-Teller distortion, (4) dynamic Jahn-Teller distortions³⁻⁶. Moreover, during delithiation, the charge compensation mechanism still seems to be under debate, especially regarding the role of oxygen over the Ni^{7,8}. There is a need for new, high-fidelity datasets that allow discrimination between these models and redox centers.

3.3.2 Multiple datasets in interaction with atomistic modelling

In the pursuit of experimental evidence, three different studies combining modelling and characterisation were performed in WP5 to understand this material.

- UCAM has combined DFT (WP2) with NMR and XRD and suggested the importance of oxygen on the charge compensation mechanism during delithiation⁹. UCAM also supported the dynamic Jahn-Teller theory¹⁰.



- Independently, CEA confirmed the role of oxygen in the charge compensation mechanism by combining DFT and HAXPES¹⁴.
- A consortium regrouping CEA, Soleil, CNRS, ESRF, Chalmers, and CNR (WP2) developed a bulk spectroscopy workflow enlisting multiple techniques on LNO samples prepared in standard conditions according to WP8 and uploaded to the BIG-MAP archive (WP9) (Figure 7)¹⁵. Indeed, operando X-ray absorption spectroscopy (XAS), operando Raman spectroscopies, ex situ hard X-ray photoelectron emission spectroscopy (HAXPES), ex situ X-ray Raman scattering (XRS), ex situ resonant inelastic X-ray scattering (RIXS) and ex situ soft XAS were performed. The collected data were analysed with the help of theoretical calculations performed in WP2 by CNR. Without going into the full ex situ Ni L-edge RIXS, bulk Ni L-edge spectra obtained by XRS, local atomic vibrations during cycling measured by operando Raman), (2) a high-fidelity dataset, since all measurements were acquired on the same sample (same level of Ni antisite defects) and cycled in similar conditions (same state of charge). Also, beam damage has been tested and ruled out. These data sets also demonstrate that oxygen is primarily responsible for the charge compensation mechanism and suggest a bond-disproportionate state for pristine LiNiO₂.

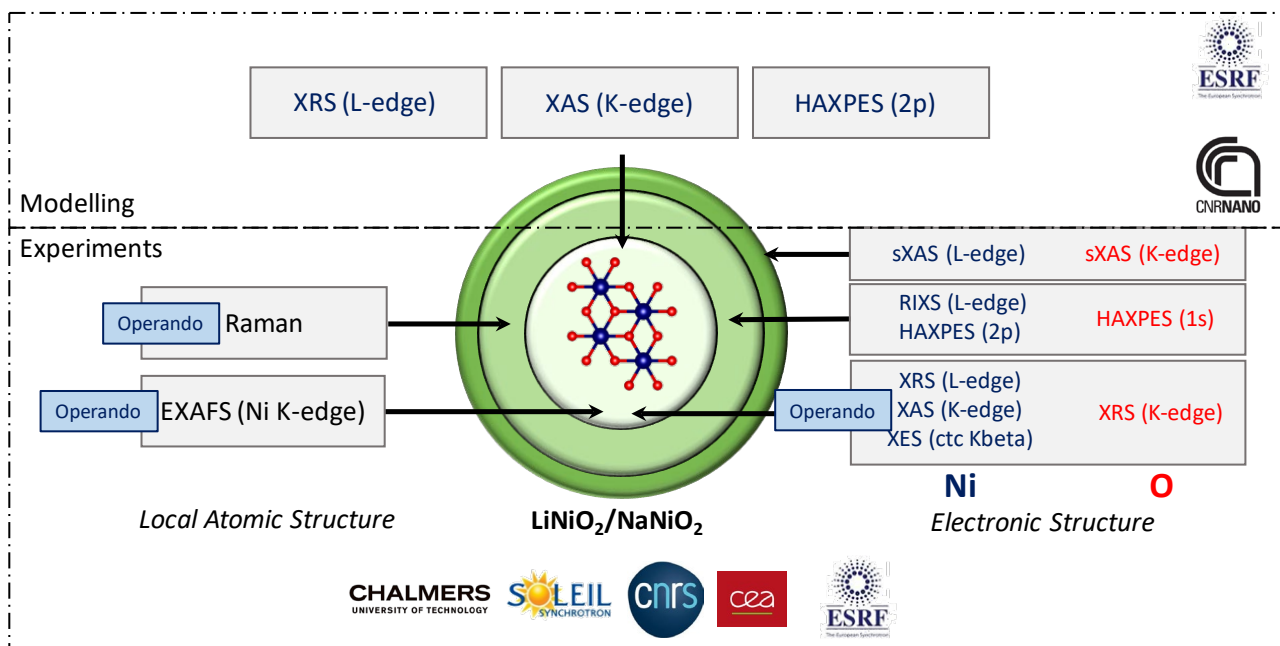


Figure 6. Bulk spectroscopy workflow enlisting new ex situ and operando datasets combined with modelling.

3.3.3 Conclusions and perspectives

Altogether, combining the different studies, there is a general agreement to define LiNiO₂ as a negative charge transfer material with electronic density around Ni similar to LiNiO₂ (Ni formally 3+) and NiO (Ni formally 2+). In the pristine state and during delithiation, electronic density around the oxygen is responsible for the charge compensation mechanism. Note that our measurements were not specifically targeted at understanding the presence of O₂ molecules, which has recently been reported¹¹. Regarding the local atomic structure of pristine LiNiO₂ (and the presence of short and long bonds), some of the work done in WP5 suggests that short and long bonds are inside the same octahedral (as in Jahn-Teller distorted systems). At the same time, other results indicate a system with long and short bonds distributed between octahedra (big and small octahedra as in a



disproportionated system). More discussions and cross-correlations between the different studies should be conducted to resolve this apparent paradox.

3.4 Demonstration of the capability to run coordinated multi-technique experiments to acquire multi-scale data and practical application to a selected chemistry

D5.3 reported a time-coordinated multi-technique and multi-scale workflow involving the collaboration of 15 partners. It is the largest workflow regarding the number of experiments performed in WP5. In short, over 30 LNO/Gr full cells with or without LiTDI additive were prepared by two partners following WP8 standard protocols. Cycled cells were disassembled, and electrodes shipped and measured in laboratories or at large-scale facilities under ex situ or operando conditions (FIB-SEM, online electrochemical mass spectrometry, NMR, TEM, and electrochemistry on model SEI, neutron imaging, TEM-EELS, neutron depth profiling, Raman mapping, operando XRD, XPS, X-ray absorption spectroscopy, Hard X-ray photoelectron spectroscopy, X-ray tomography, nano diffraction, X-ray Raman scattering, small and wide angle scattering). Experimental metadata were stored in the online BIG-MAP Notebook. The data analysis was performed using standard approaches when possible (diffraction, XPS, XAS, Raman – reported in D5.4) and stored in the BIG-MAP Archive. An AI-aided segmentation tool for tomography data analysis is also being developed with WP11 in this context (see also D5.4). The techniques were chosen to answer broad scientific questions regarding SEI and surface morphology, Li heterogeneity, electronic structure, crystalline structure, and gas reaction products. Further information is available in D5.3.

4. Definition of perspectives and future vision towards the European multi-modal platform

4.1 Introduction

In the following, we describe the future vision towards a European multi-modal platform with respect to what has been previously presented in this report. In particular, we will confront several important questions:

- How do we develop a global experimental matrix towards an automatic workflow builder?
- How do we extend workflows towards chemistry neutrality?
- Why are new access modes to large-scale facilities crucial to efficiently include these tools in workflows?
- How can data correlation be pushed further?

4.2 Towards an automatic workflow builder

Starting from the global experimental matrix, the first step would be to transition the proposed graphical user interface from a proof of concept to a finished, open tool (app), allowing one to interrogate the matrix using questions formulated in natural language. The tool would offer significant benefits in enhancing the usage of the global experimental matrix, which we consider highly valuable, for example, to industrial partners with complex characterization needs. The second step would be to have the app produce a characterization workflow from the natural language-



based question following the schematic presented in Figure 8. Ideally, the app would interrogate the BIG-MAP Archive to verify any available data. The output of the app would be threefold:

- A workflow with ordered sample preparation and experimental steps.
- A list of requirements regarding sample preparation and experiments (sample characteristics, cell specificities, etc.) to ensure successful data collection.
- General details and information regarding contact points for the experiments, instrument availability, time frames, degree of complexity for the data acquisition and processing, etc.

There are several challenges to achieving these goals. Firstly, the interface to the global experimental matrix must be improved. Secondly, constructing an algorithm would allow the selection of possible techniques and optimize the workflow according to the desired time/resource/fidelity (as discussed in D5.5). Lastly, develop an automatic search in data repositories (such as the BIG-MAP Archive) and/or fetch already available data and related publications to include them in the workflow construction process and outputs.

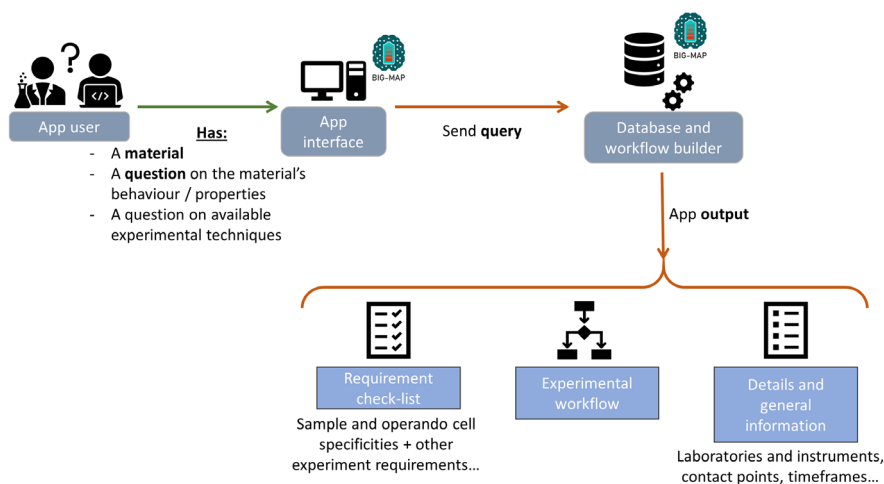


Figure 7. Schematic of the automatic workflow builder.

4.3 Extending workflows towards chemistry neutrality

The vast majority of characterization performed in WP5 have been performed on LNO (BASF) and Gr or GrSi (CIDETEC) composites using LP57 electrolyte (E-LYTE) with additives cycled in coin cells, which is, of course, a confined sub-space of the vast chemical space and cell format available in battery research. Extending the workflows is necessary to reach chemistry neutrality; however, it holds challenges:

- Large material batches of new chemistries should be available. It is essential. For example, for the sizeable aging workflow (section 3.4), approximately 50 cm² of the electrode was cycled and sent to partners (representing approx. 600 mg of active material). Producing this amount of reproducible material is not beyond the reach of most laboratories but still requires some upscaling efforts that might not be possible depending on the chemistry.
- Standard cycling protocols for relevant and reproducible electrochemistry should exist. Most ex situ characterization experiments have been conducted with samples prepared following standard electrochemical conditions. Operando experiments were performed following standard cycling protocols. These standard conditions should result from a consensus in the battery community for the selected chemistry or cell format.



- Techniques should adapt to the chemistry and cell format requirements. Some informative techniques for Li-ion batteries might not be adaptable to other chemistries. For example, neutron imaging or neutron depth profiling, being sensitive to the presence of Li, would not have the same impact on Na-ion batteries. Similarly, extending the workflows to the characterization of commercial cells would impose stringent technical requirements due to the large size of cells and the thickness of cell casings.

Therefore, we can understand that the transferability of the workflows is not straightforward or, in some cases, not advantageous. Future work could be devoted to studying this transferability and potentially adding this information to the global experimental matrix.

4.4 New access modes to large-scale facilities to facilitate the integration of these tools into efficient workflows

Large-scale facilities (LSF), such as synchrotron and neutron sources, are crucial because they give access to a multi-dimensional space of parameters from atomic scale to device scale, with ultimate temporal and spatial resolutions that make these parameters accessible during real battery operation. However, access to beam time through standard access modes is based on proposal submission designed for single-shot experiments with, in general, more than 6 months between proposal acceptance and data collection. This time scale and lack of guarantee of being able to experiment makes it very difficult to integrate these tools into timely workflows. The standard way of using large-scale facilities for complex, long-term, and strategic R&D challenges in the battery domain will need to evolve¹².

Along that line, CEA and ESRF are testing a new access mode, the Battery Pilot HUB (<https://www.esrf.fr/HUB/Battery>). The objective is to accelerate research and innovation on batteries by setting up an open scientific, technical, and communication platform dedicated to promoting, carrying out, and analysing cutting-edge synchrotron X-ray investigations of battery components and devices. For the battery research community, the HUB mechanism enables enhanced flexibility and reactivity to simultaneously tackle an array of cross-sectorial scientific questions and probe an array of samples, e.g., technological- and/or chemistry-expanded campaigns of measurements where several types of materials/batteries may be investigated in parallel and correlatively. The HUB scheme provides a novel structured approach in the field, including:

- Regular access based on long-term research programs instead of stand-alone experiments, e.g., for a structured R&D approach to advance the development of next-generation battery materials.
- Repeated access for long-term monitoring of samples and processes, e.g., for aging and degradation with cycling studies.
- Access to multiple instruments at more than one LSF with a single proposal – e.g., for multi-modal characterization of electrochemical processes on various electrode materials/battery cells.

Thanks to this new access mode, a large number of LSF experiments have been carried out by CEA in the context of the BIG-MAP project, as shown in Figure 9.

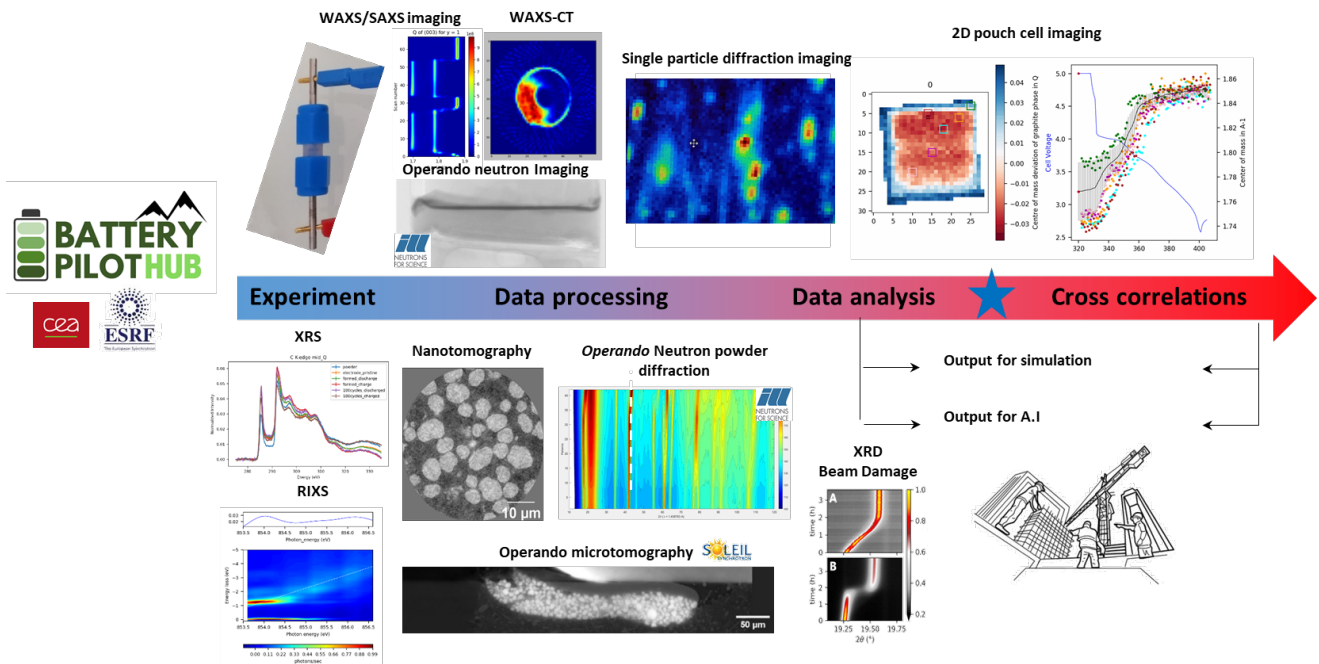


Figure 8. Graphical representation of BIG-MAP LSF experiments conducted by CEA. Most of the experiments were carried out in the framework of the Battery Pilot Hub at ESRF. Note that neutron experiments (imaging and diffraction) are made in the context of the long-term proposal between CEA and ILL (multi-instrument access proposal over several years), while the experiment at Soleil was done through a regular single proposal.

4.5 Strategies to improve data correlation

While keeping in mind that WP5 has produced vast and valuable datasets that will indeed have a substantial impact in the field, we interrogate the quality of the links between these datasets, starting with a series of critical observations:

- Results and interpretation of data originating from smaller workflows tend to be published faster. For example, several papers have been published or are currently in preparation regarding the spectroscopy of LiNiO_2 (section 3.3). In contrast, only two papers are planned for now from the sizeable aging workflow (section 3.4) due to the non-negligible work needed for data correlation.
- Correlative workflows have helped introduce new techniques to the battery community, which might not be sufficient as stand-alone experiments (for example, Ni L-edge RIXS).
- Published results from independent workflows and stand-alone experiments often agree but sometimes differ. For example, Ni anti-site mixing in LiNiO_2 varies from 2 % to 4 %. There are also differences in the interpretation of the LiNiO_2 local structure.
- Different theoretical models have been used to interpret other datasets without intercomparison in independent workflows and stand-alone experiments. For example, for the LiNiO_2 spectroscopy work, three different modelling approaches were used to interpret NMR, XPS, and bulk X-ray spectroscopy data.
- Correlation of datasets, when performed, is mainly done at the interpretation stage, with some examples of data correlation through modelling (Ni K-edge and Ni L-edge on LiNiO_2 are both compared to simulated spectra using the same theoretical model and framework).



From these observations, we learn two main points. With the current tools, increasing the amount of correlation is time-consuming but leads to more accurate results and stronger community-agreed interpretation. We believe the most efficient way of correlating datasets, for now, is in two steps: first, data are interpreted and reported in small workflows or stand-alone experiments (with details on the experimental parts and data analysis), then interpretations from the different papers are combined to report a general consortium-agreed mechanism. In WP5, for most of the scientific topics, as of the date of this report, we are at the stage in which we discuss interpretation at the consortium level. Indeed, efforts have been primarily focused on creating the first steps of the workflow process: building workflows, performing the experiments, and interpreting/publishing the first interpretations.

We foresee that accelerating data correlation is going to be one of the following challenges for setting up the European multi-modal platform, and this should rely on the following:

- Continuing to accelerate data analysis (see D5.4 for examples).
- Developing and bringing existing tools to correlated data analysis into the battery community (for example, multiple diffraction pattern refinement in Fullprof and Fullprof App¹⁶, combining spectroscopy with a total scattering in RMCProfile¹⁷ or understanding diffraction patterns from simulated microstructures with xrd_simulator¹⁸).
- Strengthening the link between modelling and experiments towards digital twins.
- Advancing the capabilities to perform AI-based recognition of correlated patterns or results

5. References (BIG-MAP references in Red):

[1] de Biasi, L.; Schiele, A.; Roca-Ayats, M.; Garcia, G.; Brezesinski, T.; Hartmann, P.; Janek, J. Phase Transformation Behavior and Stability of LiNiO₂ Cathode Material for Li-Ion Batteries Obtained from In Situ Gas Analysis and Operando X-Ray Diffraction. *ChemSusChem* 2019, 12 (10), 2240–2250.

[2] Graae, K. V.; Li, X.; Sørensen, D. R.; Ayerbe, E.; Boyano, I.; Sheptyakov, D.; Jørgensen, M. R. V.; Norby, P. Time and Space Resolved Operando Synchrotron X-Ray and Neutron Diffraction Study of NMC811/Si-Gr 5 Ah Pouch Cells. *Journal of Power Sources* 2023, 570, 232993.

[3] Foyevtsova, K.; Elfimov, I.; Rottler, J.; Sawatzky, G. A. LiNiO₂ as a High-Entropy Charge- and Bond-Disproportionated Glass. *Phys. Rev. B* 2019, 100 (16), 165104.

[4] Poletayev, A. D.; Cottom, J. P.; Morgan, B. J.; Islam, M. S. Temperature-Dependent Dynamic Disproportionation in LiNiO₂. arXiv December 8, 2022.

[5] Chung, J.-H.; Proffen, Th.; Shamoto, S.; Ghorayeb, A. M.; Croguennec, L.; Tian, W.; Sales, B. C.; Jin, R.; Mandrus, D.; Egami, T. Local Structure of LiNiO₂ Studied by Neutron Diffraction. *Phys. Rev. B* 2005, 71 (6), 064410.

[6] Sicolo, S.; Mock, M.; Bianchini, M.; Albe, K. And Yet It Moves: LiNiO₂, a Dynamic Jahn–Teller System. *Chem. Mater.* 2020, 32 (23), 10096–10103.



[7] Li, N.; Sallis, S.; Papp, J. K.; McCloskey, B. D.; Yang, W.; Tong, W. Correlating the Phase Evolution and Anionic Redox in Co-Free Ni-Rich Layered Oxide Cathodes. *Nano Energy* 2020, 78, 105365.

[8] Li, N.; Sallis, S.; Papp, J. K.; Wei, J.; McCloskey, B. D.; Yang, W.; Tong, W. Unraveling the Cationic and Anionic Redox Reactions in a Conventional Layered Oxide Cathode. *ACS Energy Lett.* 2019, 4 (12).

[9] Genreith-Schriever, A. R.; Banerjee, H.; Menon, A. S.; Basse, E. N.; Piper, L. F. J.; Grey, C. P.; Morris, A. J. Oxygen Hole Formation Controls Stability in LiNiO₂ Cathodes. *Joule* 2023, 7 (7).

[10] Genreith-Schriever, A. R.; Alexiu, A.; Phillips, G. S.; Coates, C. S.; Nagle-Cocco, L. A. V.; Bocarsly, J. D.; Sayed, F. N.; Dutton, S. E.; Grey, C. P. Jahn-Teller Distortions and Phase Transitions in LiNiO₂: Insights from Ab Initio Molecular Dynamics and Variable-Temperature X-Ray Diffraction, in preparation.

[11] Juelsholt, M.; Chen, J.; Pérez-Osorio, M. A.; Rees, G. J.; Coutinho, S. D. S.; Maynard-Casely, H. E.; Liu, J.; Everett, M.; Agrestini, S.; Garcia-Fernandez, M.; Zhou, K.-J.; House, R. A.; Bruce, P. Does Trapped O₂ Form in the Bulk of LiNiO₂ during Charging? ChemRxiv December 15, 2023.

[12] Atkins, D.; Capria, E.; Edström, K.; Famprikis, T.; Grimaud, A.; Jacquet, Q.; Johnson, M.; Matic, A.; Norby, P.; Reichert, H.; Rueff, J.-P.; Villeveille, C.; Wagemaker, M.; Lyonnard, S. Accelerating Battery Characterization Using Neutron and Synchrotron Techniques: Toward a Multi-Modal and Multi-Scale Standardized Experimental Workflow. *Advanced Energy Materials* 2022, 12 (17), 2102694.



- [13] Q. Jacquet, I. Profatlova, L. , B. Alrifai, E. Addes, P. Chassagne, N. Blanc, S. Tardif, S. Lyonnard, Correlating local structural and gas evolution: operando OEMS and WAXS/SAXS mapping, in preparation.
- [14] R. Fantin, T. Jousseume, R. Ramos, G. Lefevre, A. Van Roekeghem, J.-P. Rueff, A. Benayad, Depth-resolving the redox compensation mechanism in Li_xNiO_2 , in preparation.
- [15] A. Iadecola, Q. Jacquet, N. Mozhzhukhina, A. Matic, G. Moehl, L. Perez, J.-P. Rueff, S. Belin, F. Capone, R. Dedryvère, L. Stievano, N. B. Brookes, A. Longo, P. Gillespie, D. Prezzi, S. Lyonnard, Atomic and electronic structure of Li_xNiO_2 probed by multi - technique spectroscopies, in preparation
- [16] Rodríguez-Carvajal, J. Recent Advances in Magnetic Structure Determination by Neutron Powder Diffraction. *Physica B: Condensed Matter* **1993**, *192* (1), 55–69. [https://doi.org/10.1016/0921-4526\(93\)90108-I](https://doi.org/10.1016/0921-4526(93)90108-I).
- [17] Tucker, M. G.; Keen, D. A.; Dove, M. T.; Goodwin, A. L.; Hui, Q. RMCProfile: Reverse Monte Carlo for Polycrystalline Materials. *J. Phys.: Condens. Matter* **2007**, *19* (33), 335218. <https://doi.org/10.1088/0953-8984/19/33/335218>.
- [18] Henningsson, A.; Hall, S. A. Xrd_simulator: 3D X-Ray Diffraction Simulation Software Supporting 3D Polycrystalline Microstructure Morphology Descriptions. *J Appl Cryst* **2023**, *56* (1), 282–292. <https://doi.org/10.1107/S1600576722011001>.